

REGGE-EIKONAL APPROACH AND ITS OFF-SHELL EXTENTION VERSUS EXPERIMENTAL DATA

V. A. PETROV AND A. V. PROKUDIN

*Institute For High Energy Physics,
142284 Protvino , Russia
E-mail: petrov@mx.ihep.su
prokudin@th1.ihep.su*

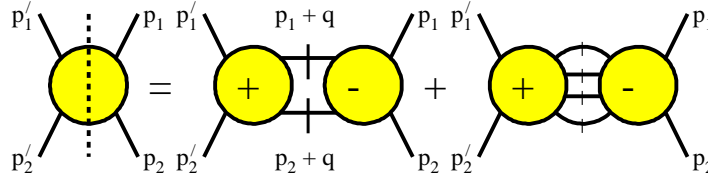
We develop an off-shell extention of the Regge-eikonal approach which automatically takes into account off-shell unitarity. We argue that exclusive vector-meson production cross-sections measured at HERA can be fairly described with classical universal Regge trajectories. No extra “hard” trajectories of high intercept are needed for that.

1 Introduction

Unitarity condition

$$ImT(s, \vec{b}) = |T(s, \vec{b})|^2 + \eta(s, \vec{b})$$

where $T(s, \vec{b})$ is the scattering amplitude in impact space representation and $\eta(s, \vec{b})$ stands for the contribution of inelastic channels, may be illustrated by the following picture in the momentum space

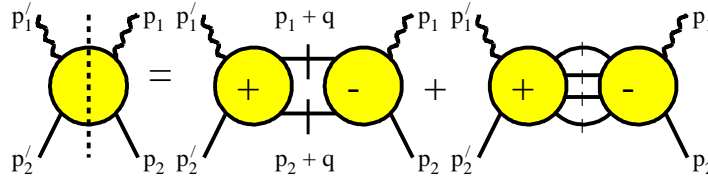


$$ImT(p_1', p_2', p_1, p_2) = \frac{-i}{(2\pi)^4} \int d^4q (-2\pi i)^2 \delta((p_1 + q)^2 - m^2) \delta((p_2 - q)^2 - m^2) \times$$

$$\times T^+(p_1 + q, p_2 - q, p'_1, p'_2) T^-(p_1, p_2, p_1 + q, p_2 - q) + \dots \quad (1)$$

where “...” stands for inelastic channels contribution.

It is worth noting that we can include virtual external particles into consideration and in this case the integration in Eq. (1) still goes over particles on mass shell as it was in the case of real external particles, i.e.



There are many parametrizations that “solve” the s -channel unitarity condition. Examples are U -matrix¹ and Eikonal approach⁴.

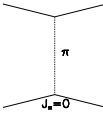
We choose the eikonal representation as usual

$$T(s, \vec{b}) = \frac{e^{2i\delta(s, \vec{b})} - 1}{2i}, \quad (2)$$

here $T(s, \vec{b})$ is the scattering amplitude, $\delta(s, \vec{b})$ is the eikonal function. The eikonal function is to be considered as a basic scattering function, which builds up the amplitude. The unitarity condition looks very simple in terms of the eikonal function:

$$Im\delta(s, \vec{b}) \geq 0, \quad s > s_{inel} \quad (3)$$

In quantum mechanics $\delta(s, \vec{b})$ is related to the (short-range) potential V :

$$\delta(s, \vec{b}) \sim \int_{-\infty}^{+\infty} dz V(z, \vec{b}) \sim$$


At relativistic energies one can generalize the notion of the potential by introducing a “quasipotential”, which is complex and depends on energy². As a concrete realization of the quasipotential one can take Van-Hove interpretation of the Regge behaviour as a “sum” of all possible one-particle exchanges in the t -channel³. Combination of the eikonal approach and Regge poles was considered for the first time in⁴. It was shown in⁵ in the framework of the asymptotic summation of the perturbative series that the eikonal function $\hat{\delta}(s, t)$ behaves like $s^{1+\Delta}$, where $\Delta > 0$.

So one could abstract the idea that there exists some function $\hat{\delta}(s, t)$ with a powerlike growth in s and this is in full conformity with general principles.

We choose the following eikonal function in t space (here t is the transferred momentum)

$$\hat{\delta}(s, t) = c \left(\frac{s}{s_0} \right)^{\alpha(0)} e^{t \frac{\rho^2}{4}} \quad (4)$$

where

$$\rho^2 = 4\alpha'(0) \ln \frac{s}{s_0} + r^2 \quad (5)$$

is referred to as a “reggeon radius”.

It means that the eikonal function has a simple pole in J plane and the corresponding Regge trajectory can be written in the following form:

$$\alpha(t) = \alpha(0) + \alpha'(0)t \quad (6)$$

We make use of linear Regge trajectories in this paper, though there exists some evidence of non-linearity of $\alpha(t)$ when t is high enough.

Functions in t - and b -spaces are related by the Fourier-Bessel transformation:

$$\begin{aligned} \hat{f}(t) &= 4\pi s \int_0^\infty db^2 J_0(b\sqrt{-t}) f(b) \\ f(b) &= \frac{1}{16\pi s} \int_{-\infty}^0 dt J_0(b\sqrt{-t}) \hat{f}(t) \end{aligned} \quad (7)$$

Making use of Eq. (7) we obtain the following b -representation of the eikonal function:

$$\delta(s, b) = \frac{c}{s_0} \left(\frac{s}{s_0} \right)^{\alpha(0)-1} e^{-\frac{b^2}{\rho^2}} \quad (8)$$

In what follows the term “pomeron” will mean the leading pole of the eikonal function.

For cross sections we use the following normalizations:

$$\begin{aligned}\sigma_{tot} &= \frac{1}{s} \text{Im} T(s, t=0) \\ \sigma_{el} &= 4\pi \int_0^\infty db^2 |T(s, b)|^2 \\ \frac{d\sigma}{dt} &= \frac{|T(s, t)|^2}{16\pi s^2}\end{aligned}\tag{9}$$

2 Regge-Eikonal Approach

Let's recall some properties of the Regge-eikonal model.

If $s \rightarrow \infty$, then

$$\sigma_{tot} \rightarrow 2\pi\rho^2 [c + \ln z - Ei(-z)]\tag{10}$$

where $z = \frac{c_0(\frac{s}{s_0})^\Delta}{2\pi\rho^2}$, here $(\Delta \equiv \alpha(0) - 1)$ and $Ei(z) = \int_{-\infty}^z \frac{e^x}{x} dx$. At extra high energies we reach the following limit:

$$\sigma_{tot} \rightarrow 8\pi\alpha'(0)\Delta \left(\ln \frac{s}{s_0}\right)^2\tag{11}$$

i.e. the powerlike behaviour of $\hat{\delta}(s, t)$ leads to the asymptotic behaviour of the full scattering amplitude which functionally saturates the Froissart-Martin bound ⁶:

$$\sigma_{tot}^{hh} \leq \frac{\pi}{m_\pi^2} \left(\ln \frac{s}{s_0}\right)^2, s \rightarrow \infty.\tag{12}$$

If $s \rightarrow \infty$, then

$$\sigma_{el} \rightarrow \pi\rho^2 [c + \ln \frac{z}{2} + Ei(-2z) - 2Ei(-z)]\tag{13}$$

and thus

$$\frac{\sigma_{el}}{\sigma_{tot}} \rightarrow \frac{1}{2}\tag{14}$$

3 The Model

In our model we choose the following contributions for the eikonal function:

$$\delta(s, b) = \delta_{\mathbb{P}}^+(s, b) + \delta_{\mathbb{Q}}^-(s, b) + \delta_f^+(s, b) + \delta_\omega^-(s, b)\tag{15}$$

where $\delta_{\mathbb{P}}^+(s, b)$ is the pomeron contribution, $\delta_{\mathbb{O}}^-(s, b)$ is the odderon^a contribution, and δ_f^+ , $\delta_{\omega}^-(s, b)$ are contributions of f meson exchange ($C = +1$) and ω meson exchange ($C = -1$).

The trajectories of f and ω are ⁷:

$$\begin{aligned}\alpha_f(t) &= 0.69 + 0.84t \\ \alpha_{\omega}(t) &= 0.47 + 0.93t\end{aligned}\tag{16}$$

and

$$\begin{aligned}\delta^+(s, b) &= [i + tg \frac{\pi(\alpha(0)-1)}{2}] \frac{c}{s_0} \left(\frac{s}{s_0}\right)^{\alpha(0)-1} \frac{e^{-\frac{b^2}{4\pi\rho^2}}}{\rho^2} \\ (C = +1) \\ \delta^-(s, b) &= [i + ctg \frac{\pi(\alpha(0)-1)}{2}] \frac{c}{s_0} \left(\frac{s}{s_0}\right)^{\alpha(0)-1} \frac{e^{-\frac{b^2}{4\pi\rho^2}}}{\rho^2} \\ (C = -1)\end{aligned}\tag{17}$$

Where $i + tg \frac{\pi(\alpha(0)-1)}{2}$ and $i + ctg \frac{\pi(\alpha(0)-1)}{2}$ are signature coefficients for $C = +1$ and $C = -1$ exchange correspondingly.

4 Fitting procedure

We explore two cases: with and without odderon contribution.

4.1 The Model With the Odderon

The results concerning the trajectories of the pomeron and the odderon are:

$$\begin{aligned}\alpha_{\mathbb{P}}(0) - 1 &= 0.11578 \pm 0.003, \quad \alpha'_{\mathbb{P}}(0) = 0.27691 \pm 0.00434 \\ \alpha_{\mathbb{O}}(0) - 1 &= 0.11578 \pm 0.00711, \quad \alpha'_{\mathbb{O}}(0) = 0.27691 \pm 0.00315\end{aligned}\tag{18}$$

where $\alpha_{\mathbb{P}}$ and $\alpha_{\mathbb{O}}$ are the intercepts of the pomeron and the odderon, $\alpha'_{\mathbb{P}}$ and $\alpha'_{\mathbb{O}}$ are the slopes of the pomeron and the odderon respectively. So the fitting procedure lead us practically to the scenario of the weakly degenerate pomeron-odderon trajectory ¹⁴.

$\alpha_{\mathbb{P}}, \alpha'_{\mathbb{P}}$ and $\alpha_{\mathbb{O}}, \alpha'_{\mathbb{O}}$ were chosen so that the following conditions of unitarity ⁸

$$\begin{aligned}\alpha_{\mathbb{P}}(0) &\geq \alpha_{\mathbb{O}}(0) \\ \alpha'_{\mathbb{P}}(0) &\geq \alpha'_{\mathbb{O}}(0)\end{aligned}\tag{19}$$

^aThe odderon is the counterpart of the pomeron with $C = -1$

would not be violated. The other parameters are in the Table.(1).

Table 1. Parameters of the model with the odderon.

$c_{\mathbb{P}}$	44.66025	$c_{\mathbb{O}}$	1.92343
c_f	241.69257	c_{ω}	71.20085
$r_{\mathbb{P}}^2(GeV^{-2})$	14.83200	$r_{\mathbb{O}}^2(GeV^{-2})$	2.18549
$r_f^2(GeV^{-2})$	5.55410	$r_{\omega}^2(GeV^{-2})$	99.99996

We find out that the odderon contribution is significant when $t \neq 0$ and it allows us to qualitatevely describe the difference in the structure of $\frac{d\sigma}{dt}$ of $\bar{p}p$ and pp 9, 10 while without this contribution we are able to describe only the slopes of $\frac{d\sigma}{dt}$ when $t = 0$.

It is worth noting that the discrepancy in the description of $\rho = \frac{ReT}{ImT}(s, t = 0)$ can be understood if we remember that the ρ data are not directly mesaured by experimentalists, but rather extracted from $\frac{d\sigma}{dt}$ experimental data in a model-dependent way.

4.2 The Model Without the Odderon

The results concerning the pomeron trajectory is:

$$\alpha_{\mathbb{P}}(0) - 1 = 0.12169 \pm 0.00286, \quad \alpha'_{\mathbb{P}}(0) = 0.20933 \pm 0.001379 \quad (20)$$

The other parameters are in the Table.(2).

Table 2. Parameters of the model without the odderon.

$c_{\mathbb{P}}$	46.599	c_{ω}	150.530
c_f	199.630		
$r_{\mathbb{P}}^2(GeV^{-2})$	21.204		
$r_f^2(GeV^{-2})$	4.872	$r_{\omega}^2(GeV^{-2})$	39.967

The intercept is slightly higher then in case of when the odderon contributes to the eikonal. As is shown, the $t = 0$ data can be described without presence of the odderon, while the $t \neq 0$ data can be described, though qualitatively only by means of the odderon. Let's remind our basic assumptions:

- Regge trajectories are linear.
- The t dependence of $\hat{\delta}(s, t)$ is exponential i.e. $\hat{\delta}(s, t) \sim e^{t\rho^2}$.

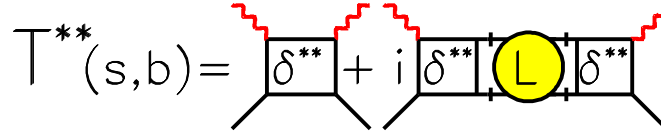
It is not our aim at present stage to obtain the best fit. What really matters is to fix a set of Regge parameters some of which are considered universal (slopes, intercepts of the trajectories) while others (residues) are not. Universal parameters will be then used for off-shell amplitudes.

5 Off-Shell Extention Of The Regge-Eikonal Approach

As it was shown in ¹⁰ the amplitude with one off-mass shell particle both in initial and final states (two asteriks) is related to the off-shell eikonals with one and two off-shell particles and on-shell amplitude in the following way

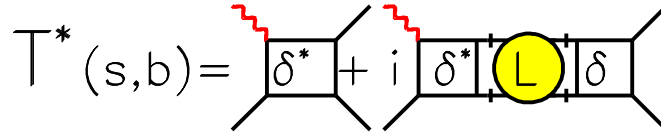
$$T^{**}(s, b) = \delta^{**}(s, b) - \frac{\delta^*(s, b)\delta^*(s, b)}{\delta(s, b)} + \frac{\delta^*(s, b)\delta^*(s, b)}{\delta(s, b)\delta(s, b)}T(s, b) \quad (21)$$

The expansion Eq. 21 can be illustrated by the following figure:



where $L = \sum_{n=2}^{\infty} \frac{(2i\delta)^{n-2}}{n!}$. The case when only one of the particles is off shell can be considered similarly. One has

$$T^* = \hat{\delta}^* + i\hat{\delta}^* \circ L \circ \hat{\delta} \quad (22)$$



or we rewrite it as follows:

$$T^*(s, b) = \frac{\delta^*(s, b)}{\delta(s, b)}T(s, b) \quad (23)$$

On the basis of Eq.(8) we take the following parametrizations of the off-shell eikonal functions:

$$\delta_{\pm}^*(s, b) = \xi_{\pm} \frac{c_*(Q^2)}{s_0 + Q^2} \left(\frac{s + Q^2}{s_0 + Q^2} \right)^{\alpha(0)-1} e^{-\frac{b^2}{\rho_*^2}} \quad (24)$$

where

$$\rho_*^2 = 4\alpha'(0) \ln \frac{s + Q^2}{s_0 + Q^2} + r_N^2 + r_*^2(Q^2) \quad (25)$$

and

$$\delta_{\pm}^{**}(s, b) = \xi_{\pm} \frac{c_{**}(Q^2)}{s_0 + Q^2} \left(\frac{s + Q^2}{s_0 + Q^2} \right)^{\alpha(0)-1} e^{-\frac{b^2}{\rho_{**}^2}} \quad (26)$$

where

$$\rho_{**}^2 = 4\alpha'(0) \ln \frac{s + Q^2}{s_0 + Q^2} + r_N^2 + r_{**}^2(Q^2) \quad (27)$$

Coefficients $c_*(Q^2)$, $c_{**}(Q^2)$ are supposed to weakly (not in a powerlike way) depend on Q^2 .

5.1 Total cross section

If we consider only the Pomeron exchange (in case of high energies, the main contribution to the scattering amplitude is due to the Pomeron) and set signature coefficient ξ_+ to be equal unity, then we have the following series for the total cross section ($\sigma_{tot}^{**} = \frac{1}{s} \text{Im} T^{**}(s, t = 0)$):

$$\sigma_{tot}^{**} = \frac{c_{**}(Q^2)}{Q^2 + s_0} \left(\frac{1}{x} \right)^{\Delta} - \frac{c_*^2 \left(\frac{1}{x} \right)^{2\Delta}}{2\pi(Q^2 + s_0)^2 \rho_*^2} \sum_{n=0}^{\infty} \frac{\left(-\frac{c(\frac{s_0}{Q^2})^{\Delta}}{2\pi s_0 \rho^2} \right)^n}{(n+2)!} \cdot \frac{\rho^2}{2\rho^2 + n\rho_*^2} \quad (28)$$

here we used the following relation $\frac{s+Q^2}{s_0+Q^2} \simeq \frac{s+Q^2-m_N^2}{Q^2} = \frac{1}{x}$ (if $s \gg Q^2$ and (or) $Q^2 \gg s_0(Q^2 \gg m_N^2)$) Now we can derive the behaviour of the total cross section in different kinematic limits:

- **Regge Regime**

$$\sigma_{tot}^{**} \rightarrow \frac{(s/Q^2)^{\Delta}}{Q^2} \left[c_{**} - \frac{c_*^2}{c} \left(\frac{s_0}{Q^2} \right)^{1+\Delta} \frac{\rho^2}{\rho_*^2} \right] \quad (29)$$

- **Bjorken Regime**

$$\sigma_{tot}^{**} \rightarrow \frac{c_{**}(Q^2)}{Q^2} \left(\frac{1}{x}\right)^\Delta - \frac{c_*^2}{2c} \cdot \frac{1}{Q^2} \cdot \left(\frac{1}{x}\right)^\Delta \cdot \left(\frac{s_o}{Q^2}\right)^{1+\Delta} \cdot \frac{\ln \frac{Q^2(1-x)}{s_o x}}{\ln \frac{1}{x}} \quad (30)$$

As we see total cross-section possesses a powerlike behaviour in the Regge limit, but this is not a violation of unitarity, as the Froissart-Martin bound⁶ cannot be proven for this case and if we put all particles on the mass shell, then we restore the ‘normal’ logarithmic asymptotical behaviour $\sigma \sim \ln^2 \frac{s}{s_0}$. In the Bjorken limit we have strong (powerlike) violation of scaling in the second term.

5.2 Elastic cross-section

For the elastic cross section we have the following expression:

$$\sigma_{el}^* = 4\pi \int_0^\infty db^2 \left| \frac{\delta^*}{\delta} T(s, b) \right|^2 \quad (31)$$

As far as $q'^2 = \mu^2$, where μ is the mass of the produced particle, it is natural to set $s_0 = \mu^2$ and now we can derive the following relations:

- **Regge Regime**

$$\sigma_{el}^* \rightarrow 16\pi\alpha'(0)\Delta \left(\frac{c_*}{c}\right)^2 \left(\frac{\mu^2}{Q^2}\right)^{2+2\Delta} (\ln \frac{s}{\mu^2})^2 \quad (32)$$

- **Bjorken Regime**

$$\sigma_{el}^* \rightarrow 8\pi\alpha'(0) \left(\frac{c_*}{c}\right)^2 \left(\frac{\mu^2}{Q^2}\right)^{2+2\Delta} \frac{(\ln(Q^2/x))^2}{\ln(1/x)} \quad (33)$$

As we can easily realize

$$\frac{\sigma_{el}^*}{\sigma_{tot}^{**}} \rightarrow 0 \quad (34)$$

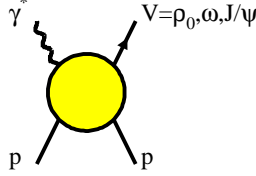
when $s \rightarrow \infty$ and $s \gg Q^2$ (compare with 14) As to the Q^2 behaviour, then as far as we have $\Delta = 0.116 \pm 0.003$ (see Eq.(18)), we obtain the following dependence:

$$\sigma_{el}^* \sim \frac{1}{(Q^2)^{2+2\Delta}} = (Q^2)^{-2.232 \pm 0.006} \quad (35)$$

This formula is in close agreement with the results of fitting the Q^2 dependence in⁹, where the power of Q^{-2} is measured as 2.24.

6 Vector meson photoproduction

For vector meson photoproduction $\gamma^* p \rightarrow V p$, where $V = \rho_0, \omega, \Phi, J/\Psi, \dots$



we have the following formula for the amplitude:

$$T^*(s, b) = \frac{\delta^*(s, b)}{\delta(s, b)} T(s, b) \quad (36)$$

here we assume that $T_{\gamma^* p \rightarrow V p} \sim T_{V^* p \rightarrow V p}$ on the basis of vector dominance¹³. As far as in this process reggeons with $C = -1$ do not contribute, we have the following contributions for the eikonal function:

$$\delta(s, b) = \delta_{\mathbb{P}}^+(s, b) + \delta_f^+(s, b) \quad (37)$$

with ($s \equiv W^2$)

$$\delta_{\pm}(W, b) = \xi_{\pm} \frac{c}{W^2 - \mu^2 - m_p^2} \left(\frac{W^2 - \mu^2 - m_p^2}{W_0^2 - \mu^2 - m_p^2} \right)^{\alpha(0)} \frac{e^{-\frac{b^2}{\rho^2}}}{4\pi\rho^2} \quad (38)$$

$$\rho^2(W) = 4\alpha'(0) \ln \frac{W^2 - \mu^2 - m_p^2}{W_0^2 - \mu^2 - m_p^2} + r_p^2 \quad (39)$$

and

$$\delta_{\pm}^*(W, b) = \xi_{\pm} \frac{c_*(Q^2)}{W^2 + Q^2 - m_p^2} \left(\frac{W^2 + Q^2 - m_p^2}{W_0^2 + Q^2 - m_p^2} \right)^{\alpha(0)} \frac{e^{-\frac{b^2}{\rho_*^2}}}{4\pi\rho_*^2} \quad (40)$$

$$\rho_*^2(W) = 4\alpha'(0) \ln \frac{W^2 + Q^2 - m_p^2}{W_0^2 + Q^2 - m_p^2} + r_p^2 + r_*^2(Q^2) \quad (41)$$

As far as Regge Eikonal approach does not constrain the Q^2 dependence of residues $c_*(Q^2)$ and radii $r_*^2(Q^2)$ we assume that the main Q^2 dependence is comprised in the other terms of our formulae and residues slowly depend

on Q^2 (they posses logarifmic behaviour)and radii depend on Q^2 as $\sim \frac{1}{Q^2}$. Eventually we have the following parametrizations:

$$c_*(Q^2) = c + c_1 \ln^3\left(\frac{Q_o^2 + Q^2}{Q_o^2}\right) \quad (42)$$

and

$$r_*^2(Q^2) = r^2 + \frac{r_1^2}{\frac{Q_o^2 + Q^2}{Q_o^2}} \quad (43)$$

where $Q_o^2 = 1.0 \text{ GeV}^2$.

The results of fitting the data to these formulae are in Fig.1.

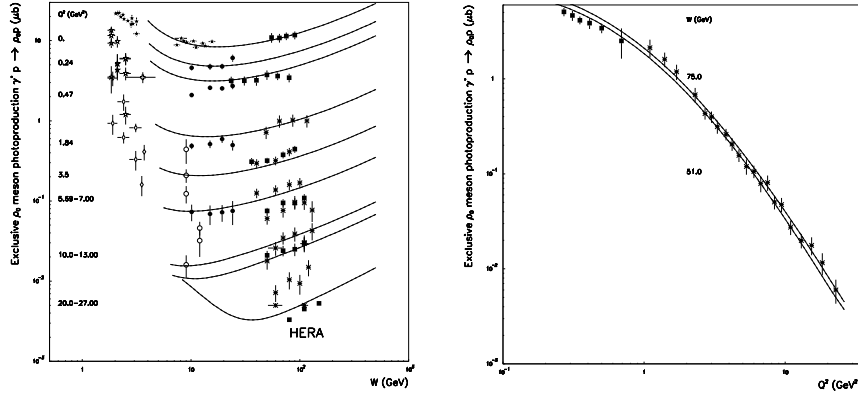


Figure 1. ρ_0 meson exclusive photoproduction cross-section

As one can see from Fig.2, in the region of energies that are available the asymptotic behaviour of exclusive vector meson photoproduction does not take place and therefore one should take into consideration both Pomeron and f meson exchanges.

For fitting we used the same intercept and slope of the pomeron that have been obtained in the Section 4.1, so that the pomeron in our model is unique and the same for all processes where it takes part.

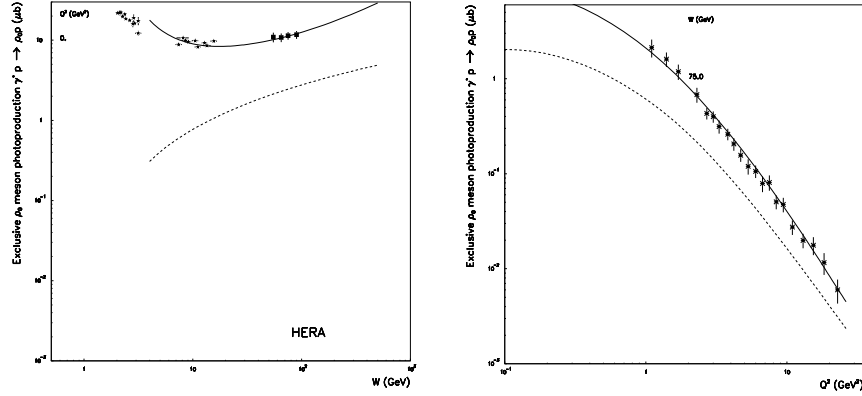


Figure 2. ρ_0 meson exclusive photoproduction cross-section (solid line)Eq. 32 in comparison with its asymptotic behaviour (dashed line) Eq. 33

7 Conclusions

As is seen from Fig.1 and Fig.2, the exclusive vector meson production may be described in the framework of extended Regge-eikonal approach and one does not need ‘hard’ pomerons with a high intercept in order to do it. The rise of cross sections when Q^2 is high is a transitory phenomenon due to effective delay of asymptotic behaviour which is observed for low Q^2 ¹¹ or ¹². The Q^2 -dependence is also described fairly well.

References

1. S. Troshin, N. Tyurin, *Yad. Fiz.* **40**, 1008 (1984).
2. A. A. Logunov A. N. Tavkhelidze , *Nuovo Cimento* **29**, 380 (1963).
3. L. Van-Hove, *Phys. Lett. B* **24**, 183 (1967).
4. R. C. Arnold, *Phys. Rev. D* **153**, 1533 (1967).
5. Cheng H., Wu T. T., *Phys. Rev. D* **186**, 1611 (1969). Cheng H., Wu T. T., *Phys. Rev. Lett.* **24**, 1456 (1970).
6. M. Froissart, *Phys. Rev. D* **123**, 1053 (1961)
A. Martin, *Phys. Rev. D* **129**, 993 (1963).

7. R. J. M. Covelan, P. Degrolard, M. Giffon, L. L. Jenkovszky, E. Predazzi, *Z. Phys. C* **58**, 109 (1993)
8. J. Finkelshtein, H. M. Fried, K. Kang, C-I Tan, *Phys. Lett. B* **232**, 257 (1989)
E. S. Martynov, *ibid.*, 367
9. C. Adloff et al., H1 Collaboration submitted to *Eur. Phys. J C*, DESY 99-010, hep-ex/9902019
10. V. A. Petrov in “Frontiers In Strong Interactions” Edited by P. Chiappetta, M. Haguenaue, J. Trân Thanh Vân. p.139
11. P. Desgrolard, A. Lengyel, E. Martynov, *Eur.Phys.J. C* **7**, 655 (1999)
12. V. Petrov, A. Prokudin, hep-ph/9706257, *Yad.Fiz* **9** 62 1 (1999)
13. N. M. Kroll, T. D. Lee, B. Zumino *Phys. Rev. D* **157**, 1376 (1967)
14. V. A. Petrov, A. P. Samokhin *Phys. Lett. B* **237**, 500 (1990)

Results of fitting without the odderon contribution

Hollow dots are pp data and full dots are $\bar{p}p$ data. The dotted (pp) and solid ($\bar{p}p$) curves correspond to the model without the odderon contribution. The shadowed area corresponds to the region available by the uncertainty in the fitting parameters.

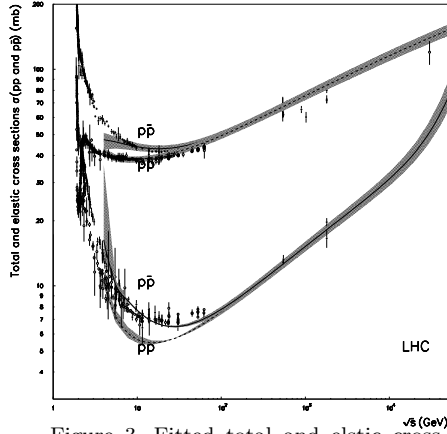


Figure 3. Fitted total and elastic cross sections.

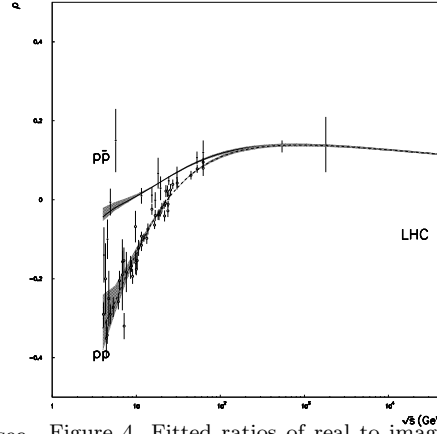


Figure 4. Fitted ratios of real to imaginary forward amplitudes.

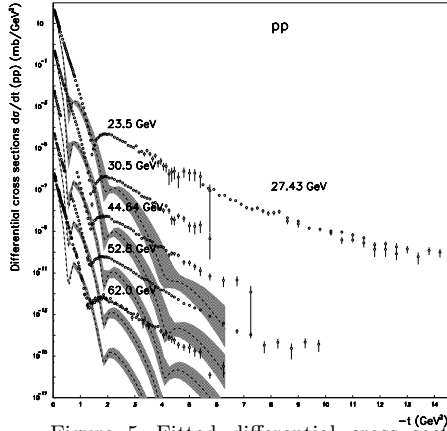


Figure 5. Fitted differential cross sections (pp).

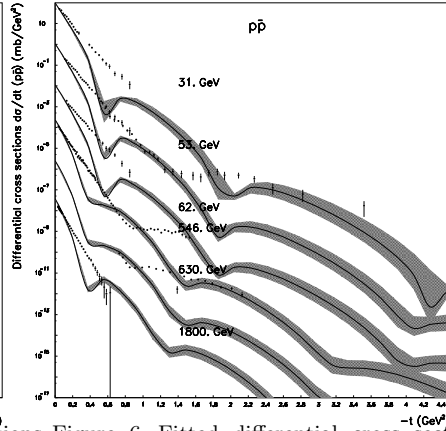


Figure 6. Fitted differential cross sections ($\bar{p}p$).

Results of fitting with the odderon contribution

Hollow dots are pp data and full dots are $\bar{p}p$ data. The dotted (pp) and solid ($\bar{p}p$) curves correspond to the model with the odderon contribution. The shadowed area corresponds to the region available by the uncertainty in the fitting parameters.

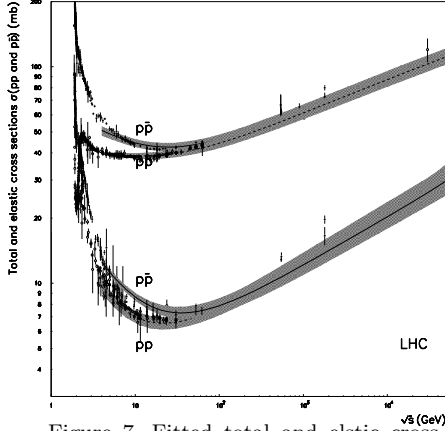


Figure 7. Fitted total and elastic cross sections.

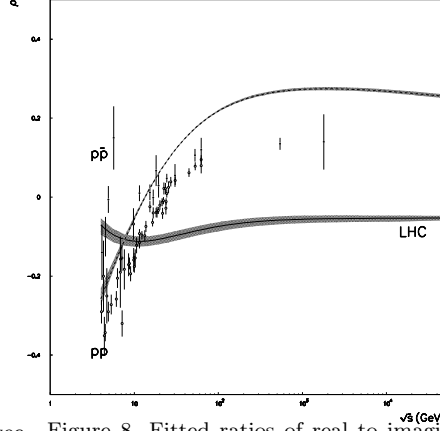


Figure 8. Fitted ratios of real to imaginary forward amplitudes.

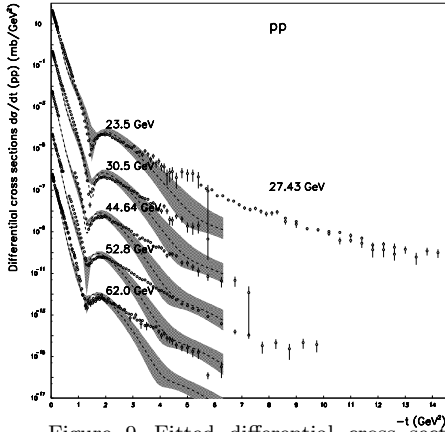


Figure 9. Fitted differential cross sections (pp).

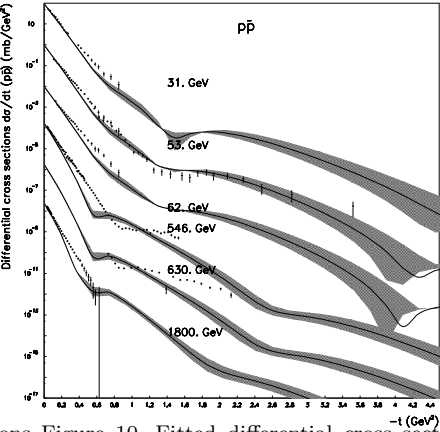


Figure 10. Fitted differential cross sections ($\bar{p}p$).